Kinetic modeling of ion conduction in KcsA potassium channel

Salvador Mafé[a] and Julio Pellicer
Departamento de Termodinàmica, Universitat de València, E-46100 Burjassot, Spain

Javier Cervera
Departamento de Ciències Experimentals, Universitat Jaume I, E-12080 Castelló, Spain

(Received 14 December 2004; accepted 23 March 2005; published online 26 May 2005)

KcsA constitutes a potassium channel of known structure that shows both high conduction rates and selectivity among monovalent cations. A kinetic model for ion conduction through this channel that assumes rapid ion transport within the filter has recently been presented by Nelson. In a recent, brief communication, we used the model to provide preliminary explanations to the experimental current-voltage *J-V* and conductance-concentration *g-S* curves obtained for a series of monovalent ions (K^+, Tl^+, and Rb^+). We did not assume rapid ion transport in the calculations, since ion transport within the selectivity filter could be rate limiting for ions other than native K^+. This previous work is now significantly extended to the following experimental problems. First, the outward rectification of the *J-V* curves in K^+ symmetrical solutions is analyzed using a generalized kinetic model. Second, the *J-V* and *g-S* curves for NH_4^+ are obtained and compared with those of other ions (the NH_4^+ *J-V* curve is qualitatively different from those of Rb^+ and Tl^+). Third, the effects of Na^+ block on K^+ and Rb^+ currents through single KcsA channels are studied and the different blocking behavior is related to the values of the translocation rate constants characteristic of ion transport within the filter. Finally, the significantly decreased K^+ conductance caused by mutation of the wild-type channel is also explained in terms of this rate constant. In order to keep the number of model parameters to a minimum, we do not allow the electrical distance (an empirical parameter of kinetic models that controls the exponential voltage dependence of the dissociation rate) to vary with the ionic species. Without introducing the relatively high number of adjustable parameters of more comprehensive site-based models, we show that ion association to the filter is rate controlling at low concentrations, but ion dissociation from the filter and ion transport within the filter could limit conduction at high concentration. Although some experimental data from other authors were included to allow qualitative comparison with model calculations, the absolute values of the effective rate constants obtained are only tentative. However, the relative changes in these constants needed to explain qualitatively the experiments should be of significance. © *2005 American Institute of Physics*. [DOI: 10.1063/1.1913502]

I. INTRODUCTION

Ion channels allow selective transport across cell membranes.[1] KcsA, a bacterial potassium channel of known structure showing both high conduction rates and selectivity among monovalent cations, has received much experimental attention recently.[2–8] Theoretical studies have addressed the origin of the channel selectivity to structureless inorganic cations and the characteristics of the concerted, multi-ion conduction mechanism through the selectivity filter (the central structural element of the channel) using molecular[9–11] and Brownian[12,13] dynamics simulations. The simulations provide atomistic level pictures that can relate structural information to observed phenomena but they involve usually time scales too short to obtain macroscopic currents[10] (except for Brownian dynamics[12,13]). On the other hand, low resolution approaches based on continuum[14] and kinetic[15] models introduce severe simplifications concerning structural aspects[15] and channel states and transitions[14] but provide useful information since electrophysiological experiments are conducted over long times compared with those on an atomic scale.[14] Atomic simulations give results coherent with classical concepts traditionally used by membrane electrophysiologists in a number of cases.[1]

Nelson has recently proposed a simple but useful kinetic model for ion permeation across open ion channels.[16–18] All microscopic configurations of the channel were represented by only three states that correspond to different ion occupancies of the selectivity filter. This is a relatively small number of states compared with previous, more complete kinetic models.[3] Simple analytical equations relating ion conduction rates with external concentrations and transmembrane voltage were obtained assuming that ion association to and dissociation from the KcsA selectivity filter (and not ion transport within this filter) can be rate limiting, with special emphasis on the case of the native K^+.[18] In a recent, brief communication, we used this model to provide preliminary explanations[19] to the experimental current-voltage, *J-V*, and conductance-concentration, g-$S(g=J/V)$, curves obtained by Miller and co-workers for the monovalent ions K^+, Tl^+, and Rb^+.[4] This previous work is now significantly extended to

[a]Electronic mail: smafe@uv.es

the following cases. First, the outward rectification in the *J-V* curves for K^+ in symmetrical solutions of different concentration is analyzed using a previous, generalized kinetic model[18] (Figs. 2 and 3). Second, the *J-V* (Figs. 4 and 5) and *g-S* (Fig. 8) curves for NH_4^+ are obtained and compared with those of other ions (the NH_4^+ *J-V* curve is qualitatively different from those of Rb^+ and Tl^+). Third, the effects of Na^+ block on K^+ and Rb^+ currents through single KcsA channels[5] are studied and the different blocking behavior is related to the rate constants characteristic of ion transport within the filter (Figs. 6 and 7). Finally, the significantly decreased K^+ conductance caused by mutation of the wild-type channel[20] is also explained in terms of this rate constant (Fig. 9).

The three-parameter model employed is distinct from that used in Ref. 18, being a mathematical simplification of the more general four-parameter model given by Nelson in the Appendix of Ref. 16. We emphasize the following differences with respect to previous approaches. First, in contrast to Ref. 18, we do not assume rapid ion transport within the filter since this could be rate limiting for ions other than K^+ [large activation energies for going around the conduction cycle among the different filter states are likely to exist in the case of Rb^+ (Ref. 3)]. Second, for the sake of simplicity, we do not allow the electrical distance δ, an empirical parameter of kinetic models that controls the exponential voltage dependence of the dissociation rate constants, to vary with the ion.[18] Electrical distances give valuable information but they are not free of criticisms.[14] In the case of K^+, the distances obtained when fitting theory to experiment may be reasonable, with $\delta=0.15$ as a typical value.[16,18] However, preliminary fittings for other ions gave $\delta=0.3$ for Rb^+ and $\delta=0.01$ for Tl^+ (see Table 1 in Ref. 18). These distances differ by a factor of 30 for the narrow, 1.2 nm long selectivity filter.[7] Moreover, the value of δ for Rb^+ is relatively close to that of K^+ but significantly different from that of Tl^+ while the experimental *J-V* curves are sublinear for K^+ and Tl^+ but superlinear for Rb^+.[4,18] The fact is that electrical distances could not have a simple structural interpretation for the case of concerted multi-ion transport.[21] Therefore, we have assumed that $\delta=0$ for all ions as a first approximation and based our analysis on the relative values of the rate constants needed to interpret the experimental data. The conduction steps that determine the transport of ions other than the native K^+ ion are then studied without forcing the electrical distance to assume rather extreme values.

II. MODEL EQUATIONS

Figure 1 shows the conduction steps in the selectivity filter.[16,19] Experimental and simulation studies[2,3,6,10] suggest that two K^+ ions separated by a single water molecule shift back and forth between the inner (i) and outer (o) configurations. The incorporation of a third ion from the solution causes the exit of a different ion from the opposite side. Simulation shows that repulsive forces are essential for high conduction rates[11] since they allow the affinity that each ion has for its binding site to be overcome[8] (note that the two positive ions are the "countercharges" for the negative charges of the oxygen atoms in the selectivity filter[7]). When

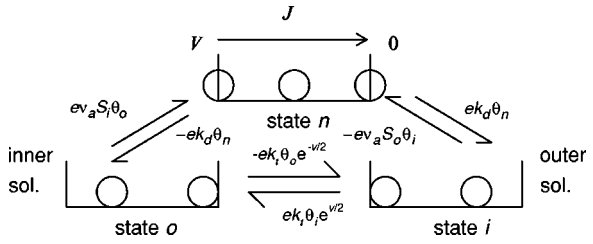

FIG. 1. Schematic view of the conduction steps in the ion channel according to Nelson (Ref. 16). We do not assume rapid ion translocation for all ions and introduce $\delta=0$ (Ref. 19).

the system is in the transition state n, an ion can leave the filter. Ion association to the filter in states o and i is rate controlling at low concentrations but dissociation from the filter in state n and the translocation step between states i and o (or the equivalent transport mechanism in the filter for ions other than K^+) could limit conduction at high concentrations. Note that introducing $\delta=0$ is equivalent to assume that neither the association nor the dissociation rate constants are voltage dependent. This assumption could not be valid for quantitative studies,[5,16,18] but it allows to show the role of the different conduction steps using a minimum number of model parameters.

The states of Fig. 1 incorporate the central elements of the channel revealed by KcsA structural data,[3,8] although the vestibule outside the selectivity filter should also be included in more refined models.[2,5,10,11] Although experiments and simulations show that conformational changes and fluctuations[7,10,11] could be important, incorporation of the filter flexibility is out of the scope of the present model. Note also that the significant changes in the filter structure at low K^+ concentration are not likely to occur in the high concentration conduction cycle.[7,8] We do not imply that the protein is in anyway rigid at the short time scale but rather than the filter should have some average, well-defined spatial structure over the long times characteristic of conduction. It is clear that the filter must experience some structural changes as K^+ ions translocate between states i and o but the structural adjustments should be relatively small in this case.[7,8] Finally, in order to focus our study on the different conduction mechanisms that characterize each particular ion, the two different concentration-dependent permeation modes[18] that could be present in the case of K^+ will not be considered here.

According to the model of Fig. 1, the ion currents J can be obtained from the system of equations[16,19]

$$J = e\nu_a S_i \theta_o - ek_d \theta_n, \tag{1a}$$

$$J = ek_d \theta_n - e\nu_a S_o \theta_i, \tag{1b}$$

$$J = ek_t e^{v/2} \theta_i - ek_t e^{-v/2} \theta_o. \tag{1c}$$

In Eq. (1c), the ion concentrations are $S_i=S_o=S$ for symmetrical solutions and the probabilities of finding the channel in the states of Fig. 1 are related by $\theta_i+\theta_o+\theta_n=1$. Also, $v=eV/kT$ is the dimensionless transmembrane voltage, where k is the Boltzmann constant, T is the absolute temperature, and e is the proton charge. Since most of the applied voltage

falls across the filter,[2,21,22] V is the potential difference between the filter ends approximately. Finally, ν_a and k_d are the voltage-independent association and dissociation rate constants, respectively, and k_t is the rate constant characteristic of ion transport within the filter. The association rate constant includes both transport (diffusion to the filter) and sorption (dehydration) limitations. The energy landscape and structural periodicity experienced by each particular ion-water queue in the filter[3,7] are lumped into the single rate constant k_t. Note that if the concerted translocation step in Fig. 1 were to apply only to K^+ but not to other ions (e.g., Rb^+), k_t would not then be the translocation rate constant between configurations i and o in this case, but an effective rate constant characteristic of the particular ion transport mechanism within the selectivity filter (as opposed to the association ν_a and dissociation k_d rate constants that characterize interfacial transfer phenomena). The kinetic model[16,18] in Fig. 1 can be compared with a previous approach by Schumaker and Mackinnon.[23,24]

Equations (1a)–(1c) constitute a mathematical simplification of the complete, more general four-parameter (ν_a, k_d, k_t, and δ) model given in the Appendix of Ref. 16. However, Nelson chose to analyze the effects of ν_a, k_d, and δ instead of those of ν_a, k_d, and k_t considered here. This difference is not trivial: the use of finite values for the rate constant k_t can explain the sublinear and superlinear behaviors observed in the J-V curves for the different ions without introducing dramatically different values for δ. Moreover, the values used for k_t can be justified in terms of the different conduction mechanisms within the selectivity filter. Therefore, the present study constitutes a significant addition to previous work where preliminary fittings were attempted.[18]

The J-V curve that results from Eqs. (1a)–(1c) is

$$J = 2e\nu_a S \sinh(v/2)\left(\frac{k_d}{\nu_a S + 2k_d}\right)\left(\frac{k_t}{\nu_a S + 2k_t \cosh(v/2)}\right). \tag{2a}$$

If transport within the filter is not rate limiting ($k_t \gg \nu_a S$), Eq. (2a) simplifies to

$$J = ek_d \tanh(v/2)\left(\frac{S}{S + (2k_d/\nu_a)}\right). \tag{2b}$$

If dissociation is not rate limiting ($k_d \gg \nu_a S$), Eq. (2a) simplifies to

$$J = ek_t \sinh(v/2)\left(\frac{S}{S + (2k_t/\nu_a)\cosh(v/2)}\right). \tag{2c}$$

Although Eqs. (2b) and (2c) can be transformed into universal Michaelis–Menten functions of a reduced concentration, this is not the case of the more general Eq. (2a).[16,18] Therefore, since the Michaelis–Menten kinetics is approximately valid for most channels,[1,16,18] the extreme limiting case where $k_t \ll \nu_a S$ and $k_d \ll \nu_a S$ simultaneously in Eq. (2a) should not occur frequently. In this case the probability of the transient state would be exceedingly high, $\theta_n \approx 1 \gg \theta_i \approx \theta_0 \approx 0$, and J would then decrease rather than increase with S; actually, the transient state n in Fig. 1 should not be so frequent because of electrostatic repulsion, but this question is ignored in the model. We will analyze the above case later when discussing Fig. 8.

Equation (2b) constitutes a reasonable approximation for those ions (e.g., K^+) showing rapid, concerted single-file motion in either direction. On the contrary, Eq. (2c) should be more appropriate for other ions (e.g., Rb^+) where the suboptimal structural periodicity of the water-ion queue makes concerted translocation between states o and i of Fig. 1 more difficult[7] and other transport mechanisms within the filter could be operative. The more general Eq. (2a) may apply to ions having intermediate properties as well as to those showing rapid transport within the filter if the concentration is so high that the condition $k_t \gg \nu_a S$ is no longer valid. Note finally that the association step is always rate limiting at low concentrations: Eqs. (2b) and (2c) give a linear behavior of J with S for low S.

III. RESULTS AND DISCUSSION

To study the different ion conduction mechanisms present in Eqs. (2a)–(2c), we will assign values to the kinetic rate constants ν_a, k_d, and k_t for each ion. The currents observed for different concentrations and transmembrane voltages allow to estimate the rate constants characteristic of each experimental regime. For example, the observed current at low concentration (where ion association is rate limiting) provides a first estimation of the association constant v_a for an extensive concentration range. A similar procedure can be followed to obtain the dissociation k_d or translocation k_t constants at high concentrations (where ion association is no longer rate limiting) and high voltages. Finally, for the translocation step (or the equivalent transport mechanism within the filter) to be rate limiting, k_t and k_d should take similar values. Considering simultaneously the J-V and g-S curves allow a more stringent estimation of the rate constants. Although the absolute values of these effective rate constants are tentative only, the relative changes in the constants needed to explain qualitatively the experiments are of significance and could be correlated to the occupancy in the selectivity filter.

Computer simulations show typical times of only 0.5 ns for K^+ motion between adjacent sites, with a time scale much higher in the case of Na^+,[10] but ion transport across the full selectivity filter can take a longer time because it involves several atomic steps. Experimental studies[3,4] give K^+ currents in the range 1–40 pA for ionic concentrations in the range 20–800 mM and transmembrane voltages in the range 20–200 mV. The observed currents are lower for other permeant ions (NH_4^+, Rb^+, and Tl^+) and much lower for Na^+. The rate constants characteristic of each experimental regime can be estimated from the above values, as explained above. (When fitting the experimental data[4] to his phenomenological model, Nelson found $\nu_a = 6 \times 10^8 M^{-1} s^{-1}$ and $k_d = 2 \times 10^8 s^{-1}$ for K^+ assuming a voltage dependence to the dissociation rate constants.[18])

Although the above estimations are significant, the rate constants include so many effects (ionic diffusion to the filter, dehydration, transport between sites, dissociation from the filter, rehydration) lumped into two or three single num-

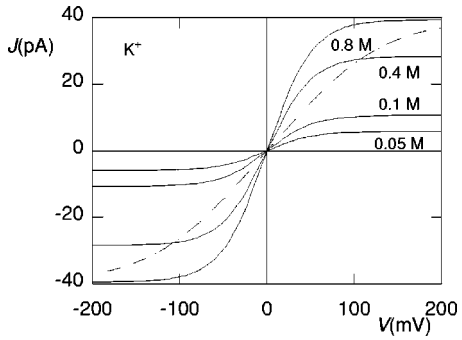

FIG. 2. *J-V* curves for K^+ symmetrical solutions of different concentration *S* obtained from Eq. (2b) with $\nu_a=16\times10^8$ M^{-1} s^{-1} and $k_d=4\times10^8$ s^{-1} (Ref. 19). The dashed curve with $S=0.8M$ corresponds to conduction when both ion dissociation from and transport within the filter are rate limiting [Eq. (2a) with $k_t\approx k_d$].

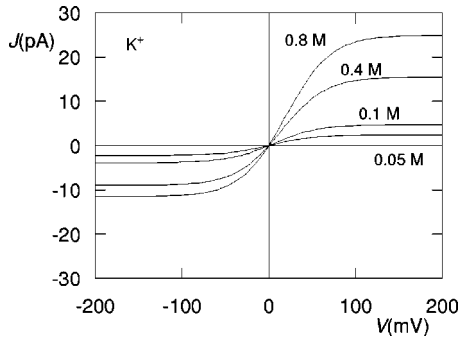

FIG. 3. *J-V* curves for K^+ symmetrical solutions of different concentration *S* obtained from Eq. (3a) for $k_i=0.25k_o$, with $\nu_o=\nu_a$ and $k_o=k_d$ as in Fig. 2. Outward rectification increases with K^+ concentration.

bers that their absolute values are rather crude. We will emphasize only the relative changes in the rate constants needed to explain qualitatively the *J-V* curves.[4,18] (The same rate constants should be able to describe also the *g-S* curves.[3,4]) Therefore, reference to a particular ion in the calculations is made only to emphasize the qualitative differences between the experimental curves reflecting different conduction mechanisms. Quantitative studies would need more elaborated models with a higher number of channel states[3] and parameters[18] as well as more extensive experimental data.[4]

Figure 2 shows the *J-V* curves obtained for K^+ at different concentrations using Eq. (2b) with[19] $\nu_a=16\times10^8M^{-1}\,s^{-1}$ and $k_d=4\times10^8s^{-1}$. The dashed curve corresponds to conduction when both ion dissociation from and transport within the filter are rate limiting [Eq. (2a) with $k_t\approx k_d$]. This could be the case of rapid translocation if the concentration is so high that Eq. (2b) is not a good approximation to Eq. (2a). When the results of Fig. 2 are compared with the experimental data in Figs. 1 and 2 of Ref. 4, it is observed that the use of a third parameter (k_t) in the *J-V* curve appears to show a better qualitative agreement to experiment at high salt concentrations: The saturation of current with potential *V* is not so marked in the experiments[4] at high *S* as in the continuous curves of Fig. 2. However, in contrast to the theoretical results of Fig. 2, the experiments show weak outward rectification.[4]

Although the ability of the filter to show concerted, K^+ single-file motion in either direction may suggest the absence of rectification effects, asymmetric open channel *J-V* curves can still result from differences between the water-filled central cavity and the channel side bathed by the extracellular solution.[2,3] It is difficult to correct for rectification effects because of both experimental and theoretical questions. Indeed, LeMasurier *et al.* stated that above 800 mM K^+, open probability becomes so low that full *J-V* curves could not be measured (see the caption of Fig. 2 in Ref. 4). Moreover, the model does not explicitly account for the access resistance, which can be important for electrical potentials higher than 100 mV approximately (see, e.g., Fig. 4a of Ref. 13). Finally, rectification effects may also arise because of an asymmetric distribution of the fixed charges in the intracellular and extracellular entryways. The negatively charged, acidic amino acids in these regions[2,6] can give (asymmetric) ion concentrations and *p*H values different from those in the (symmetrical) external solutions. It is noteworthy that some channels which have a similar filter to KcsA show actually different rectification properties.[6,18]

Despite the above problems, rectification effects will tentatively be addressed here by introducing asymmetric values to ν_a and k_d in Eqs. (1a) and (1b). Nelson has generalized his kinetic model to the case of asymmetric channels with different values of the rate constants.[18] However, he analyzed the effects associated with asymmetric electrical distances δ instead of those associated with the rate constants ν_a and k_d considered here. The resulting *J-V* curve that generalizes Eq. (2b) for $k_o\neq k_i$ is

$$J=ek_o\frac{1-e^{-v}}{1+(k_o/k_i)e^{-v}}\frac{c^*}{1+c^*},$$
$$c^*=2S\frac{1+(k_o/k_i)e^{-v}}{(1+e^{-v})(2k_o/\nu_o)[1+(k_o/k_i)]}, \tag{3a}$$

where subscripts *o* and *i* in the rate constants make reference to the outer and inner ends of the selectivity filter. We have assumed that $k_o/k_i=\nu_o/\nu_i$ because of the symmetry of the selectivity filter.[18] Consider now the following limiting cases of Eq. (3a) at high transmembrane voltages $|v|\gg1$. For low concentrations ($c^*\ll1$), we obtain the symmetric behavior

$$J=\pm eS\left(\frac{\nu_o\nu_i}{\nu_o+\nu_i}\right), \tag{3b}$$

where positive (negative) currents correspond to positive (negative) values of *V*. For high concentrations ($c^*\gg1$), however, Eq. (3a) gives the asymmetric fluxes

$$J(V>0)=ek_o\neq|-ek_i|=|J(V<0)|. \tag{3c}$$

Therefore, in the limit of high transmembrane voltages, ion association to the filter occurs with the (effective) symmetrical rate constant of Eq. (3b), being rate limiting at low concentrations. On the contrary, ion dissociation from the filter occurs with the asymmetric rate constants of Eq. (3c), being rate limiting at high concentrations. Current rectification should therefore be expected in the latter case, as it is observed experimentally.[4]

Figure 3 shows the *J-V* curves for K^+ symmetrical solu-

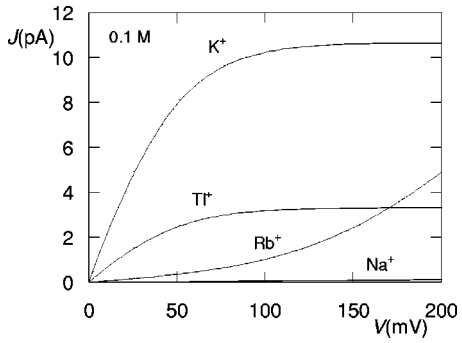

FIG. 4. *J-V* curves for K^+, Tl^+, Rb^+, and Na^+ in symmetrical solutions of ionic concentration $S=0.1M$, (Ref. 19). The K^+ curve is obtained from Eq. (2b) as in Fig. 2. The Tl^+ curve is also obtained from Eq. (2b), but now with $\nu_a(Tl^+)=\nu_a(K^+)$ and $k_d(Tl^+)=0.07k_d(K^+)$. For Rb^+, we use Eq. (2c) instead of Eq. (2b) with $\nu_a(Rb^+)=\nu_a(K^+)$ and $k_t(Rb^+)=0.005k_d(K^+)$. Finally, for Na^+ we employ also Eq. (2c) but now with $\nu_a(Na^+)=0.01\nu_a(K^+)$ and $k_t(Na^+)=0.0005k_d(K^+)$.

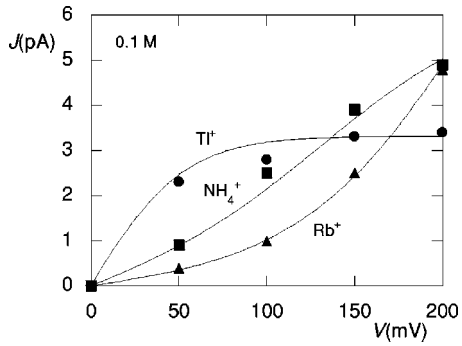

FIG. 5. *J-V* curves for NH_4^+, Tl^+, and Rb^+ in symmetrical solutions of ionic concentration $S=0.1M$ for voltages $V>0$. The NH_4^+ curve is obtained from Eq. (2c) with $\nu_a(NH_4^+)=0.5\nu_a(Rb^+)$ and $k_t(NH_4^+)=3k_t(Rb^+)$. The experimental data are typical of Tl^+ (circles), Rb^+ (triangles), and NH_4^+ (squares) in Fig. 4 of Ref. 4.

tions of different concentration S obtained using Eq. (3a) for $k_i=0.25k_o$ with $\nu_o=\nu_a$ and $k_o=k_d$ as in Fig. 2. Outward rectification increases as K^+ concentration increases, in qualitative agreement with the experimental results in Figs. 1 and 2 of Ref. 4. Although many phenomena may influence the measured *J-V* curves,[4] asymmetric rate constants could result from differences between the water-filled central cavity (inner end of the selectivity filter) and the channel side bathed by the extracellular solution (outer end of the selectivity filter).[2,3] These structural differences are also present in the Na^+ block of the channel[4,5] as well as in the *J-V* curves for all permeant ions.[4] Indeed, Fig. 4 of Ref. 4 shows weak outward rectification for all ions although the detailed curve shape differs for each species (almost linear, sublinear, and superlinear behaviors of J with V are observed). We will focus next on the different shapes of the experimental *J-V* curves. Some experimental data from Ref. 4 are included to allow comparison with the model calculations (these data were directly read from the published original figures and constitute therefore approximated values).

Figure 4 presents the *J-V* curves obtained for different sets of rate constants intended to be representative of ions K^+, Tl^+, Rb^+, and Na^+ in symmetrical solutions of concentration $S=0.1M$.[19] The K^+ curve is obtained from Eq. (2b) as in Fig. 2. The Tl^+ curve is also obtained from Eq. (2b), but now with $\nu_a(Tl^+)=\nu_a(K^+)$ and $k_d(Tl^+)=0.07k_d(K^+)$ (this value differs slightly from that used in Ref. 19), since Tl^+ is a tightly binding ion[7] that should not be able to leave the filter as readily as K^+ does (In this context, bi-ionic permeability studies based on reversal potentials determined from *J-V* curves show that Tl^+, the least conductive of the permeant ions, is the most "permeant," a circumstance associated with tightly binding permeating ions in both cation and anion channels.[4]) In contrast to the case of Tl^+ where the structural periodicity of the ion-water queue appears to follow closely that of K^+, the periodicity is suboptimal in the case of Rb^+.[7] Therefore, although this ion is also able to enter the filter, transport within the filter can be now rate limiting. Consequently, the Rb^+ curve is obtained using Eq. (2c) instead of Eq. (2b) with $\nu_a(Rb^+)=\nu_a(K^+)$ but $k_t(Rb^+)=0.005k_d(K^+)$. Although not shown in Fig. 4, it is remarkable that Eq. (2c) switches from superlinear to sublinear behavior at very high voltages (as it will be shown in Fig. 6 later), in agreement with recent experimental data[5] that show voltage-independent currents suggesting diffusion-limited transport when $V>300$ mV.

The *J-V* curves for Na^+ are also obtained from Eq. (2c) with $\nu_a(Na^+)=0.01\nu_a(K^+)$ and $k_t(Na^+)=0.0005k_d(K^+)$ to account for the fact that K^+ transport rates exceed those of Na^+ by several orders of magnitude[8] (Fig. 7 of Ref. 4 clearly shows the lack of Na^+ permeability from *J-V* curves obtained under mixing ion conditions). This gives approximately $J(Na^+)\approx 0.01J(K^+)$ in Fig. 4, which can be decreased further by decreasing $\nu_a(Na^+)$. The Na^+ conduction rates would also be negligible if we were to use Eq. (2b) instead of Eq. (2c) provided that $k_d(Na^+)\approx k_t(Na^+)$, although it is clear that the two conduction mechanisms are qualitatively different. We have used Eq. (2c) instead of Eq. (2b) here because recent molecular dynamics simulations show that in contrast to K^+, Na^+ does not exhibit rapid translocation.[10]

The theoretical results in Fig. 4 correctly describe the experimental superlinear (Rb^+) and sublinear (Tl^+) *J-V* curves observed in Fig. 4 of Ref. 4. In particular, it is not necessary to assume that the dissociation step is rate limiting to explain the apparently surprising Rb^+ superlinear curve[18] if we consider that it is the process characteristic of Rb^+ transport within the selectivity filter that limits conduction[3,5] in this case. This process, characterized here by an effective rate constant k_t, should be different from the K^+ concerted translocation. According to the model calculations, the native K^+ may maximize conduction rates with respect to other monovalent ions through high association (compared with Na^+), high translocation (compared with Rb^+), and high dissociation (compared with Tl^+) rates. In this case, all the rate constants in the product $\nu_a S k_t k_d$ of Eq. (2a) can achieve high values simultaneously.

Interestingly, the experimental *J-V* curve for NH_4^+ in Fig. 4 of Ref. 4 shows a more linear behavior, being qualitatively different from those for Rb^+ and Tl^+.[4] Indeed, NH_4^+ appears to follow an intermediate behavior between those of Rb^+ [obtained with Eq. (2c)] and Tl^+ [obtained with Eq. (2b)], as shown in Fig. 5. Therefore, this behavior might be qualitatively reproduced using the more complete Eq. (2a) to which

Eqs. (2b) and (2c) are limiting approximations. However, it could also approximately be obtained with Eq. (2c) forcing the rate constants ν_a and k_t to take lower and higher values, respectively, than those characteristic of Rb^+. Figure 5 shows the *J*-*V* curves for NH_4^+, Tl^+, and Rb^+ in symmetrical solutions of ionic concentration $S=0.1M$ for voltages $V>0$. Typical experimental data from Ref. 4 are included to allow comparison to the theoretical curves. The NH_4^+ curve, calculated using Eq. (2c) with $\nu_a=0.5\nu_a(Rb^+)$ and $k_t=3k_t(Rb^+)$, follows the slightly curved, *s*-shaped experimental points. Unfortunately, the relevant microscopic information available for Rb^+ and Tl^+ (Refs. 2,3,7) is lacking here, although the rate constants used for NH_4^+ are close to those of Rb^+ that has a similar ionic radius. (Note that the rate constants used in the calculations of Figs. 4 and 5 are not assigned completely *ad hoc*: they are related to microscopic information whenever available.)

A recent experimental study[5] analyzed the effects of Na^+ block on K^+ and Rb^+ currents through single KcsA channels, and concluded that the different blocking behavior observed can be correlated with the inhomogeneous energetic landscape of Rb^+ in the selectivity filter.[3] The capability of K^+ to switch from the *o* and *i* states in Fig. 1, in contrast to Rb^+, could explain the remarkable voltage dependence of Na^+ block in K^+ compared with Rb^+ which shows instead an *s*-shaped, steady increase of *J* with *V*. Indeed, Fig. 3 of Ref. 5 shows that at low voltages ($V<100$ mV), Na^+ is not able to enter the filter and therefore the K^+*J*-*V* curve is similar to that in the absence of the blocking ion (see Fig. 2). However, at higher voltages ($100\ \text{mV}<V<200\ \text{mV}$) *J* begins to decrease rather than increase with *V*. This experimental finding is explained in terms of Na^+ inclusion within the filter.[5] To describe quantitatively this effect, we should introduce additional current equations for Na^+ together with a higher number of (mixing) ion occupancy states with voltage-dependent binding constants. This is a formidable task that requires the introduction of additional assumptions and parameters.[5]

We wish to gain some insight into this problem within the limited scope of the present model. We could assume that if inclusion of Na^+ disturbs the K^+ concerted translocation between the *i* and *o* configurations, this should decrease the effective value of k_t and, according to Eq. (2a), give low values of *J*. (The dashed curve of Fig. 2 clearly shows that decreasing the value of k_t causes the K^+ current to decrease significantly.) For high voltages ($V>200$ mV), however, the K^+ current rises again in Fig. 3 of Ref. 5, which suggests that Na^+ can now be forced through the selectivity filter. The clearance of Na^+ would resume the K^+ translocation,[5] with the concomitant increases of both k_t and *J* in the model considered here.

To analyze theoretically the Na^+ blocking, consider first the case of Rb^+. In order to include the effects of Na^+ block on the *J*-*V* curves for Rb^+, we substitute $\nu_a/(1+K_BB)$ for ν_a in Eq. (2c) where K_B and *B* are the Na^+ binding constant and concentration, respectively. Figure 6 shows the *J*-*V* curves for Rb^+ in symmetrical solutions of concentration $S=0.1M$ for voltages $V>0$. The numbers in the curves are the blocking ion (Na^+) concentrations, with $K_B=10M^{-1}$. The theoretical curves correctly capture the experimental trends in

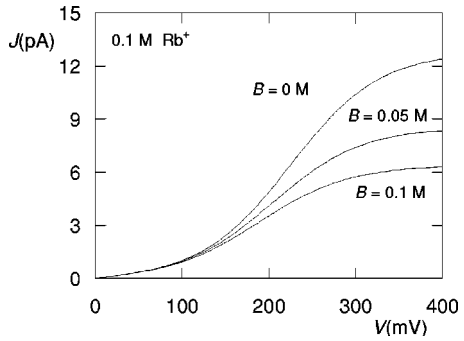

FIG. 6. *J*-*V* curves for Rb^+ in symmetrical solutions of ionic concentration $S=0.1M$ for voltages $V>0$. The rate constants are the same as Fig. 4 except that we substitute $\nu_a/(1+K_BB)$ for ν_a in Eq. (2c) where K_B and *B* are the Na^+ binding constant and concentration, respectively. The numbers in the curves are the blocking ion (Na^+) concentrations with $K_B=10M^{-1}$.

Figs. 4 and 5 of Ref. 5 that show a *s*-shaped increase of *J* with *V*. Remarkably, Na^+ block reduces the Rb^+ current without changing the general shape of the *J*-*V* curve. However, the above theoretical procedure should not be valid for K^+ because inclusion of Na^+ in the filter disturbs the K^+ switch between the *o* and *i* states in Fig. 1, in contrast to Rb^+.[5] Therefore, we keep ν_a in Eq. (2a) as in Fig. 2 in the case of K^+ but decrease now the value of k_t to mimic the inhibition of K^+ concerted transport when Na^+ substitutes for one of the two K^+ ions in the filter. When compared to the Rb^+ case, this theoretical procedure allows to show the different effects of rate constants ν_a and k_t in Eqs. (2a) and (2c), respectively (for quantitative studies, however, it is clear that both rate constants should be decreased in the case of K^+).

Figure 7 shows the resulting *J*-*V* curves in K^+ symmetrical solutions of ionic concentration $S=0.1M$ for voltages $V>0$. The downward arrow schematically shows the effect of Na^+ incorporation to the filter (note that concerted translocation requires K^+-K^+ pairs to be much more frequent than Na^+-K^+ pairs to be operative). The upward arrow is intended to show the effect of Na^+ clearance from the filter and resuming of K^+ concerted translocation, with the concomitant increase in k_t. Obviously, the present model is completely unable to quantitatively describe the experimental results (note that the different curves in Fig. 7 are obtained by

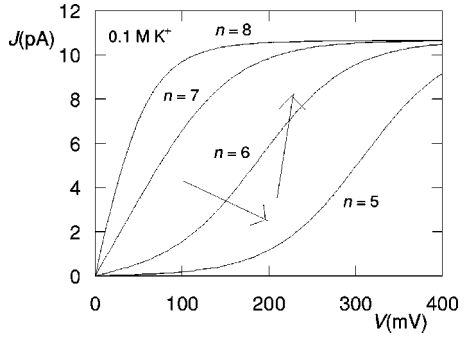

FIG. 7. *J*-*V* curves for K^+ in symmetrical solutions of ionic concentration $S=0.1M$ for voltages $V>0$. The curves correspond to different values of the translocation rate constant $k_t=4\times10^n\text{s}^{-1}$ ($n=5$, 6, 7, and 8) with ν_a as in Fig. 2. The downward and upward arrows are intended to schematically show the effects of Na^+ incorporation to and clearance from the filter (and resuming of K^+ concerted translocation), respectively.

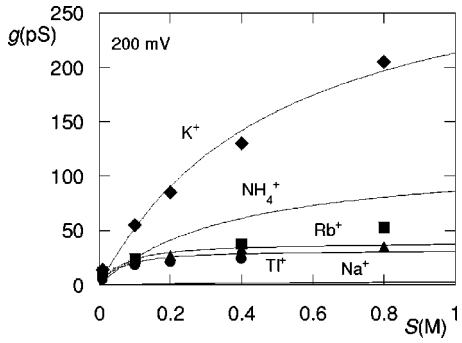

FIG. 8. g-S curves for K^+, NH_4^+, Rb^+, Tl^+, and Na^+ in symmetrical solutions of ionic concentration S at transmembrane voltage $V=200$ mV for the same rate constants of Figs. 4 and 5. The experimental data are typical of K^+ (rhombus), Tl^+ (circles), Rb^+ (triangles), and NH_4^+ (squares) in Figs. 3 and 5 of Ref. 4.

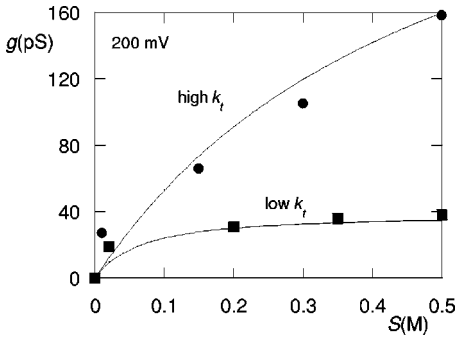

FIG. 9. g-S curves for high and low values of rate constant k_t at transmembrane voltage $V=200$ mV with the same rate constants of Fig. 4. The experimental data correspond to the wild-type (points) and mutant (squares) channels in Fig. 4 of Ref. 20.

changing only a single number, the rate constant k_t). This was done in Ref. 5 using an extensive number of channel states and transitions together with a set of concentration-dependent fitting parameters in the voltage-dependent binding constants for the different ions. However, it is apparent in Figs. 6 and 7 that the effect of Na^+ block on the J-V curve should be qualitatively different if Na^+ inclusion decreases the translocation rate constant k_t (the case of K^+) and not only the association rate constant ν_a (the case of Rb^+). In particular, if k_t in Eq. (2a) takes values close to those characteristic of Rb^+, K^+ transport within the filter can become rate limiting and the concavity of the J-V curve for K^+ shifts to that of Rb^+ (compare Fig. 7 with Fig. 4 where the different concavities are shown). Therefore, although the voltage-dependent kinetics is much more complex in the presence of Na^+ block[5] than in the trivial case assumed in the calculations, some qualitative insights may still be given by lumping together the additional effects present in the problem into an effective, voltage-dependent translocation constant for K^+.

Figure 8 shows the g-S curves for ions K^+, NH_4^+, Rb^+, Tl^+, and Na^+ in symmetrical solutions of concentration S at transmembrane voltage $V=200$ mV with the same rate constants of Figs. 4 and 5. Typical experimental data from Ref. 4 are included (again, these data were read directly from the original published figures and constitute therefore approximated values) to allow comparison with the theoretical curves. There is a rapid increase of conductance at low concentrations that is more evident for K^+ than for the other ions, followed by a tendency to saturation at high concentration. These trends are reproduced by the theoretical curves of the model. In particular, the conductances are similar at low concentrations but differ significantly when S increases, in agreement with the experimental data, which shows that the association step is rate limiting at low concentrations. Indeed, Eq. (2b) predicts a linear behavior of g with S when $k_d \gg \nu_a S$ and this is also the case of Eq. (2c) when $k_t \gg \nu_a S$.

For concentrations high enough, however, the extreme limiting case where $k_t \ll \nu_a S$ and $k_d \ll \nu_a S$ simultaneously in Eq. (2a) occurs. In this situation, the probability of the transient state is exceedingly high ($\theta_n \approx 1 \gg \theta_i \approx \theta_o \approx 0$) and g decreases rather than increases with S (not shown in Fig. 8). This effect has been noted previously.[24] When the ion concentration is so high that the association rate exceeds the translocation rate, exit from one side of the filter is followed by re-entry of an ion from the same side. Therefore, translocation is greatly diminished and this reduces both the net cycling rate and the conductance.[24] Remarkably, conductance maxima have experimentally been observed in some channels and explained by Schumaker and Mackinnon using models conceptually similar to that considered here.[23,24]

It should be noted that traditional continuum theories based on the Nernst–Planck equation with the Goldman constant field assumption[1] could not deal easily with the single-file, concerted multi-ion transport in the filter. In the case of symmetrical solutions, these theories would naturally lead to curves more linear than those of Figs. 4 and 8, although it is true that introduction of additional refinements can improve significantly the theoretical predictions.[14] In the present model, Eq. (2a) [and its limiting case, Eq. (2c), for certain values of the rate constants] can give J-V curves that are intermediate between the sublinear and superlinear curves of Eqs. (2b) and (2c) over a range of voltages if we admit that ion conduction can also be limited by transport within the filter (see the dashed curve in Fig. 2 as well as Fig. 5).

The conductance of a mutant KcsA K^+ channel with altered selectivity filter ion distribution and conduction properties has recently been studied.[20] The mutation significantly changes the K^+ conductance with respect to wild-type channel. Experimental data from Fig. 4 of Ref. 20 are included in Fig. 9. These data show that the tendency to conductance saturation of K^+ at high concentrations is more marked in the mutant than in the wild-type channel (remarkably, the g-S curve of K^+ in the mutant channel is similar to that of Rb^+ in Fig. 8). However, this is not the case of Rb^+, which shows a similar tendency to saturation in both the wild-type and the mutant channels (see Fig. 6 of Ref. 20). Moreover, Fig. 4 of Ref. 20 shows that the experimental J-V curve for K^+ switches from sublinear (wild-type channel) to superlinear (mutant channel) after mutation. On the contrary, Fig. 6 of Ref. 20 shows that the experimental J-V curve for Rb^+ remains almost unchanged after mutation (note that concerted translocation is not operative for Rb^+).

The above experimental findings can tentatively be re-

lated to changes in the K^+ translocation constant. If according to Ref. 20 mutation destroys the energetic balance between the states *o* and *i* of Fig. 1, the translocation rate constant k_t for K^+ in the mutant channel should be significantly decreased with respect to the wild-type channel (this effect should be less noticeable for Rb^+, which lacks concerted translocation). As noted in Figs. 4 and 8, the decrease of k_t causes qualitative changes in the theoretical *J-V* and *g-S* curves that closely follow those experimentally reported. In the case of the *J-V* curve, Fig. 4 shows that if k_t in Eq. (2a) is decreased to values close to those characteristic of Rb^+, K^+ transport within the filter can become rate limiting, and the concavity of the *J-V* curve for K^+ shifts to that characteristic of Rb^+ (the K^+ sublinear behavior becomes now superlinear, in agreement with Fig. 4 of Ref. 20). In the case of the *g-S* curve, Fig. 9 shows the theoretical results for high and low values of k_t at transmembrane voltage $V=200$ mV with the same rate constants of Fig. 8. Clearly, the tendency to conductance saturation at high concentrations is more marked in the curve with low k_t, which should correspond here to the mutant channel.

IV. CONCLUSIONS

We have given qualitative explanations to the experimental *J-V* and *g-S* curves of KcsA channel obtained recently for a series of monovalent ions.[4] To this end, we have employed a kinetic model by Nelson[16] without assuming rapid translocation for all ions[19] and paying special attention to the consequences of finite transport rates within the selectivity filter. In an attempt to clearly show which are the central concepts of the problem, we have kept the number of rate constants to a minimum, without introducing the relatively high number of parameters that appear in more complete kinetic models with many channel states and sites. Although some experimental data from other authors were included to allow qualitative comparison with model calculations, we believe that the fitting of a particular, limited set of experimental data is not essential for the model to be useful. Indeed, the limited number of microscopic characteristics included in the model precludes its application to quantitative analysis. However, the relative changes needed to explain the qualitative features of the *J-V* curves for each particular ion should be of significance. Quantitative analysis would need more elaborated models, with a higher number of channel states[3,5] and voltage-dependent rate constants,[16,18] together with more comprehensive experimental data.[4,5] In particular, further studies could address the higher-order coupling between ion fluxes in opposite directions,[16] the case of ionic mixtures resulting in anomalous conduction behavior[4] and the voltage-dependent Na^+ block on K^+ currents.[5]

ACKNOWLEDGMENTS

Financial support from the CICYT, Ministerio de Ciencia y Tecnologia, under Project Nos. MAT2005-01441 and FIS2004-03424, and the Fondo Europeo para el Desarrollo regional (FEDER) is acknowledged. The authors are grateful to Professor José A. Manzanares, Universitat de València, for helpful discussions.

[1] B. Hille, *Ion Channels of Excitable Membranes*, 3rd ed. (Sinauer Associates, Sunderland, MA, 2001); D. P. Tieleman, P. C. Biggin, G. R. Smith, and M. S. P. Sansom, Q. Rev. Biophys. **34**, 473 (2001); S. H. Chung and S. Kuyucak, Biochim. Biophys. Acta **1565**, 267 (2002); D. Gillespie, W. Nonner, and R. S. Eisenberg, J. Phys.: Condens. Matter **14**, 12129 (2002); G. V. Miloshevsky and P. C. Jordan, Trends Neurosci. **27**, 308 (2004).
[2] A. Doyle, J. H. Morais-Cabral, R. A. Pfuetzner, A. Kuo, J. M. Gulbis, S. L. Cohen, B. T. Chait, and R. Mackinnon, Science **280**, 69 (1998).
[3] H. Morais-Cabral, Y. Zhou, and R. Mackinnon, Nature (London) **414**, 37 (2001).
[4] M. LeMasurier, L. Heginbotham, and C. Miller, J. Gen. Physiol. **118**, 303 (2001).
[5] C. M. Nimigean and C. Miller, J. Gen. Physiol. **120**, 323 (2002).
[6] C. M. Nimigean, J. S. Chappie, and C. Miller, Biochemistry **42**, 9263 (2003).
[7] Y. Zhou and R. Mackinnon, J. Mol. Biol. **333**, 965 (2003).
[8] R. Mackinnon, FEBS Lett. **555**, 62 (2003).
[9] J. Aqvist and V. Luzhkov, Nature (London) **404**, 881 (2000).
[10] S. Bernèche and B. Roux, Nature (London) **414**, 73 (2001).
[11] I. H. Shrisvastava, D. P. Tieleman, P. C. Biggin, and M. S. P. Sansom, Biophys. J. **83**, 633 (2002).
[12] T. W. Allen, S. Kuyucak, and S. H. Chung, Biophys. J. **77**, 2502 (1999); J. Chem. Phys. **112**, 8191 (2000); T. W. Allen and S. H. Chung, Biochim. Biophys. Acta **1515**, 83 (2001).
[13] S. Bernèche and B. Roux, Proc. Natl. Acad. Sci. U.S.A. **100**, 8644 (2003).
[14] W. Nonner, D. P. Chen, and B. Eisenberg, J. Gen. Physiol. **113**, 773 (1999).
[15] C. Miller, J. Gen. Physiol. **113**, 783 (1999).
[16] P. H. Nelson, J. Chem. Phys. **117**, 11396 (2002).
[17] P. H. Nelson, J. Chem. Phys. **119**, 6981 (2003).
[18] P. H. Nelson, Phys. Rev. E **68**, 061908 (2003).
[19] S. Mafé and J. Pellicer, Phys. Rev. E **71**, 022901 (2005).
[20] M. Zhou and R. Mackinnon, J. Mol. Biol. **338**, 839 (2004).
[21] Y. Jiang and R. Mackinnon, J. Gen. Physiol. **115**, 269 (2000).
[22] Y. Jiang, A. Lee, J. Chen, M. Cadene, B. T. Chait, and R. Mackinnon, Nature (London) **417**, 523 (2002).
[23] M. F. Schumaker and R. Mackinnon, Biophys. J. **58**, 975 (1990).
[24] Z. Lu and R. Mackinnon, J. Gen. Physiol. **104**, 477 (1994).